

Finite element modelling of transmission line structures under tornado wind loading

A. Hamada^{1a}, A.A. El Damatty^{*1b}, H. Hangan^{2c} and A.Y. Shehata^{3d}

¹*Department of Civil and Environmental Engineering, Faculty of Engineering,
The University of Western Ontario, London, Ontario, Canada N6A 5B9*

²*Alan G. Davenport Wind Engineering Group, The Boundary Layer Wind Tunnel Laboratory,
Faculty of Engineering, The University of Western Ontario, London, Ontario, Canada*

³*Atomic Energy of Canada Limited, Mississauga, Ontario, Canada*

(Received November 10, 2009, Accepted March 9, 2010)

Abstract. The majority of weather-related failures of transmission line structures that have occurred in the past have been attributed to high intensity localized wind events, in the form of tornadoes and downbursts. A numerical scheme is developed in the current study to assess the performance of transmission lines under tornado wind load events. The tornado wind field is based on a model scale Computational Fluid Dynamic (CFD) analysis that was conducted and validated in a previous study. Using field measurements and code specifications, the CFD model data is used to estimate the wind fields for F4 and F2 full scale tornadoes. The wind forces associated with these tornado fields are evaluated and later incorporated into a nonlinear finite element three-dimensional model for the transmission line system, which includes a simulation for the towers and the conductors. A comparison is carried between the forces in the members resulting from the tornadoes, and those obtained using the conventional design wind loads. The study reveals the importance of considering tornadoes when designing transmission line structures.

Keywords: tornado; finite element; transmission line; transmission tower; wind load.

1. Introduction

Localized severe wind events in the form of tornadoes, downbursts and microburst are referred to as “High Intensity Wind (HIW) events”. Such events are believed to be responsible for more than 80% of all weather-related transmission line failures worldwide. Despite this fact, the codes of practice and design for transmission line structures are based on the wind loads resulting from large-scale synoptic events. The vertical profile of the boundary layer wind of a large-scale event is characterized by a monotonic increase in velocity with height. Such a profile is different than the velocity profiles of tornadoes. In addition, a significant vertical velocity component exists in the case of tornadoes. The

* Corresponding Author, Professor, E-mail: damatty@uwo.ca

^aMaster of Engineering Science Student

^bProfessor

^cAssociate Professor

^dStructural Engineer

current study focuses on assessing the response of transmission line structures to tornado loading.

The complexity in analyzing transmission line structures under HIW arises from the fact that the forces acting on the tower and the conductors vary according to the location of the event relative to the tower. This is due to the localized nature of these events. Also, depending on the location of the event relative to the tower, various spans of conductors can be subjected to different, and in some cases, uneven distribution of wind loads. This can lead to a resultant longitudinal force (parallel to the conductors) acting on the tower cross-arms. HIW events, such as tornadoes, are short-lived localized surface vortex flows that originate from thunderstorms. They have a severe rotating column of air that extends from the clouds to the earth. The tornado path width can reach up to 500 (m); therefore, field measurements are difficult to obtain and are poorly defined. Recently, field measurements were introduced by Sarkar *et al.* (2005) for the 1998 Spencer South Dakota F4 tornado and by Lee and Wurman (2005) for the 1999 Mulhall F4 tornado. Doppler radar was used to obtain the tornado field measurements. However, the recorded data is not very accurate for the near ground region (for height less than 50 (m)). Due to the complexity and difficulty of obtaining full-scale data, especially for the near ground region, laboratory simulations are used. These include the Tornado Vortex Chambers (TVC), in which tornadoes are represented as vortices. The TVC's provide a good simulation of the characteristics inside a tornado, but the results are sensitive and are affected by the applied boundary conditions. For the near ground region, numerical simulations can be done using fluid dynamics software, such as the commercial program FLUENT (Fluent Inc. 2005). Numerical simulations can provide a good assessment of the flow field near the ground.

Few studies related to the behaviour of transmission lines under HIW events are available in the literature. The modelling and assessment of the behaviour of transmission lines under downburst loading were conducted by Shehata *et al.* (2005) and Shehata and El Damatty (2007). The failure of a transmission tower during a downburst event, which occurred in Manitoba, Canada in 1996, was assessed by Shehata and El Damatty (2008). The failure of a self supported lattice tower under tornado and microburst wind profiles was investigated by Savory *et al.* (2001). The analysis was done for the tower alone, without modelling the transmission lines, and without considering the vertical velocity component. Chay *et al.* (2007) studied the dynamic response of a guyed transmission line tower under time domain simulated boundary layer and downburst winds. The wind models included turbulence. Only the radial component is taken into consideration in the study due to the insignificant effect of the vertical component of downburst. The study discussed the significant variation in the levels of response of the guyed transmission tower for the different wind loading cases, showing the importance of using specific response factors based on the type of loading.

In the current study, the numerical model developed by Hangan and Kim (2008) and the field data recorded by Sarkar *et al.* (2005) are used to estimate the wind velocity profile for both F4 and F2 tornadoes. Both an axisymmetric and a three dimensional profile are considered. The spatial variation of those wind fields are described in this paper. To the best of the authors' knowledge, the only CFD data for tornadoes available in the literature was obtained from the study conducted by Hangan and Kim (2008). This set of data is given in a steady-state manner, i.e., has no variation in time. It has the advantage of providing a good match with full-scale tornado measurements. No turbulence model is included in this set of data. For downbursts, Shehata *et al.* (2005) evaluated the natural periods of same transmission line considered in the current study, and recommended to proceed with static analysis, due to the significant difference between the period of loading and the natural periods of the structure. Chay *et al.* (2007) investigated the dynamic behaviour of transmission line system taking into account the turbulent component of downbursts. Savory *et al.* (2001)

investigated a self-supported tower under the mean velocity component of a translating tornado. They reached the conclusion that the dynamic analysis gave the same results as the static analysis. It can be concluded from previous studies that no significant dynamic effect occur when turbulence is not included in the analysis of transmission lines under high intensity wind loading. Due to the lack of a turbulence model for tornadoes, and also in view of previous findings, the analysis is conducted in this study in a static manner. A static, elastic and geometric nonlinear finite element model is developed, simulating the structural behaviour of the towers and the conductors. The nonlinear behaviour of the conductors, including the pretension and sagging effects, is included in the model. The velocity profiles mentioned above, associated with F4 and F2 scale tornadoes are incorporated into the finite element simulation. Details of the numerical model are described, including steps conducted to estimate the wind loads. A case study for a guyed transmission line system is considered. Forces that develop in selected members of the tower due to both the F4 and F2 tornadoes are evaluated. They are compared to the corresponding forces associated with normal wind loads, based on the ASCE No. 74 guideline (1991).

2. Tornado CFD numerical model

The velocity wind field associated with tornadoes used in this study is obtained from a three-dimensional Computational Fluid Dynamic (CFD) simulation conducted by Hangan and Kim (2008). The CFD simulation was conducted using the commercial program FLUENT (Fluent Inc. 2005). The simulations of tornado-like vortices included the formation of a laminar vortex at low swirl ratio, followed by turbulent vortex breakdowns and vortex touch downs at higher swirl ratio values. A schematic of the computational domain is shown in Fig. 1. In this figure, r_o and h_o are the radius and height of the computational domain, respectively.

The boundary conditions applied in the CFD analysis are shown in Fig. 1. At the inlet, a boundary layer profile is assumed for the radial velocity, V_r , and the tangential velocity, V_t , that are described by Eqs. (1) and (2), respectively

$$V_r(z) = V_o \times (z/z_o)^{\frac{1}{7}} \quad (1)$$

$$V_t(z) = 2 \times S \times V_r(z) \quad (2)$$

Where: V_o = reference velocity, z_o = reference height and S (swirl ratio) = $0.5 V_t/V_r$.

In the simulation, values of 0.3 m/sec and 0.025 m were assumed for V_o and z_o , respectively. More details about the CFD simulation including the applied turbulence model can be found at Hangan and Kim (2008).

The simulation was initially conducted using a value of $S = 0.28$. This is the same swirl ratio applied in the experimental program conducted by Baker (1981) using a Ward-type vortex chamber. The results of the CFD analysis with $S = 0.28$ were validated by Hangan and Kim (2008) through a comparison with Baker (1981) experimental results. The numerical analysis was then extended by Hangan and Kim (2008) by considering values of $S = 0.10, 0.4, 0.7, 0.8, 1.0$ and 2.0 , respectively. It should be noted that the CFD analysis was conducted at steady-state manner and, therefore, the resulting velocity field has no variation with time. The velocity field resulting from the CFD analysis $V_m(r, \theta, z)$ has a three dimensional spatial variation and is given as a function of the cylindrical coordinates r, θ and z .

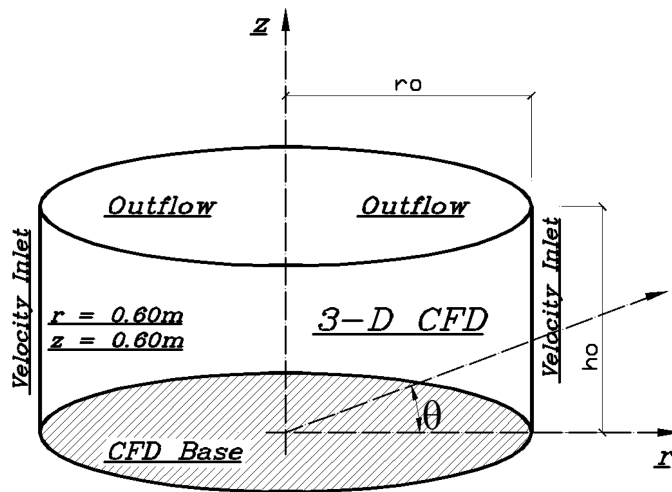


Fig. 1 Computational domain for the 3-D simulations of tornadoes

An averaging of data is conducted along the circumference, eliminating the variation of the velocity profile with θ , and leading to an axisymmetric set of data $V_m(r, z)$. Both the 3-D and the axisymmetric set of data is used in the analysis conducted in this study. It should be noted that the velocity field $V_m(r, \theta, z)$ has three velocity components: the radial $V_{mr}(r, \theta, z)$, the tangential $V_{mt}(r, \theta, z)$ and the axial $V_{ma}(r, \theta, z)$. Similar components exist for the axisymmetric velocity profile.

3. F4 – Tornado wind field

Full scale data for the F4 tornado, which occurred in Spencer, South Dakota, USA, in May 30, 1998, was recorded by Wurman (1998) using the “Doppler on Wheels” system (DOW). This set of tornado field measurements was also presented by Sarkar *et al.* (2005). The measurements predicted that the maximum tangential velocity had a magnitude of 142 (m/sec) and occurred at coordinates $r = 158$ (m) and $z = 28$ (m), where r is the radial distance relative to the tornado centre and z is the vertical distance relative to ground. An extensive study was conducted by Hangan and Kim (2008) to estimate the proper swirl ratio that should be applied to the numerical model in order to obtain good matching between the numerical results and the F4 tornado field measurements. Also, the proper length scale (L_s) and velocity scale (V_s), to be applied to the CFD data in order to simulate the F4 tornado, were obtained in this study. Hangan and Kim (2008) found that the values of $S = 2$, $L_s = 4000$ and, $V_s = 13$ provided a very good match between the scaled CFD data and the field measurements, in terms of the radial profile of the tangential velocity. These scaling factors are applied to the 3-D and the axisymmetric data to obtain 3-D and axisymmetric velocity fields simulating F4 tornadoes.

The magnitude and location of the maximum values of the three velocity components of the axisymmetric velocity field are provided in Table 1. The tabulated values indicate that the radial and axial components are significantly less than the tangential component. The ratio between the maximum radial and maximum tangential component is about 1:2. Also, it can be noticed that the maximum values of the three components occur at three different locations.

In order to gain an insight into the F4 tornado wind field, various vertical profiles for the

Table 1 Peak values and corresponding location for the velocity components for F4 and F2 tornadoes

Tornado	Direction	Velocity(m/sec)	r(m)	z(m)
F4	Peak tangential	142	158	28
	Peak radial	-79	273	7
	Peak axial	62	246	158
F2	Peak tangential	78	96	19
	Peak radial	-49	146	6
	Peak axial	37	171	127

tangential velocity component of the axisymmetric data are provided in Fig. 2. As shown in the figure, the vertical profiles are provided at various radial distances “r”.

The following observations can be drawn from the plot:

- For radial distance $r \leq 300$ (m), the profile is different than the conventional boundary wind profile, which is typically characterized by a monotonic increase of the velocity with height. For values of $r > 300$ (m), the tornado profile becomes similar to the boundary layer profile.
- For very small values of r , the vertical location of the peak values becomes very close to the ground. The vertical location of the peak value increases with the increase of r . At $r = 200$ (m), the peak value occurs at a height of about 50 (m).
- The absolute maximum tangential velocity of 142 (m/sec) occurs at $r = 158$ (m) and $z = 28$ (m), agreeing with the values given in Table 1.

The vertical profiles of the radial and the axial components, corresponding to the location of maximum tangential velocity $V = 142$ (m/sec), are plotted in Fig. 3. The vertical profile of the tangential component is provided in the same figure for comparison. The following observations can be drawn from this figure:

- The peak value of the radial component occurs very close to ground.

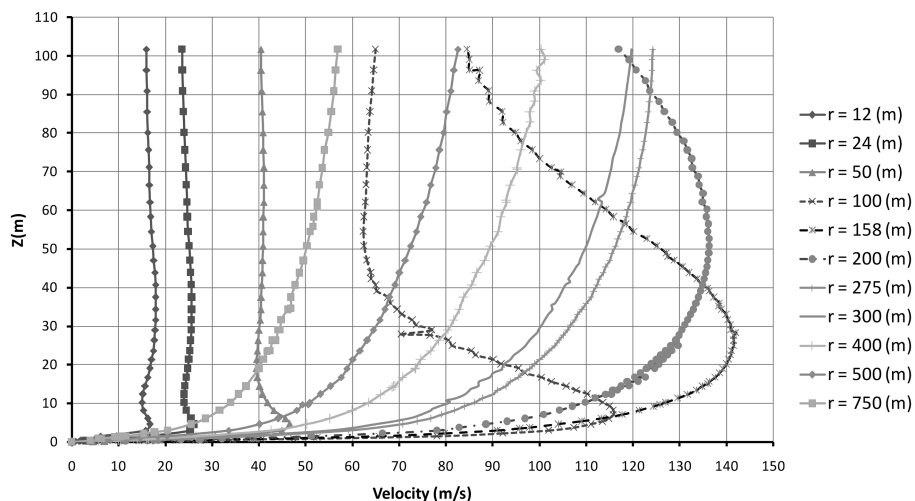


Fig. 2 Vertical profile of tangential component for different radial distances from tornado centre (F4 Tornado)

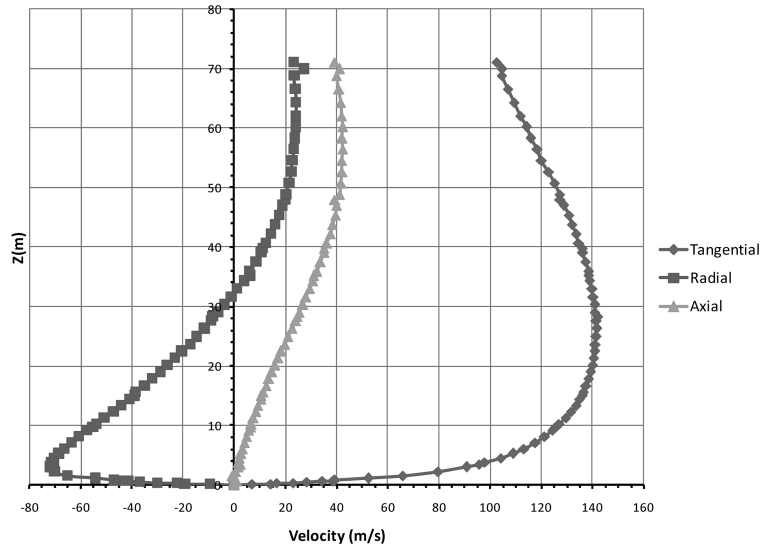


Fig. 3 Variation of the three velocity components of F4 tornado along the height at $r = 158$ (m)

- At a height $z < 30$ (m), the radial component has a negative value, i.e., acts in an inward direction. Beyond this height (i.e., for $z > 30$ (m)), the radial component acts along the outward direction.
- The axial component acts in an upward direction. It is also characterized by a zero value at $z = 0$ and a gradual increase in the velocity with height.

The near-to-centre velocity profile indicates the occurrence of vortex instability in this region. As a demonstration, the vertical profile of the three velocity components for $r = 100$ (m) is provided in Fig. 4. The peak radial velocity is located near the ground and has a negative value (inward). The direction of the radial component changes along the height from inward to outward. This component almost vanishes for heights greater than 70 (m). Also, the direction of the axial component varies along the height. It acts in an upward direction near the ground and switches to a downward direction at an elevation of 50 (m).

An assessment of the difference between the axisymmetric and the 3-D CFD data is conducted. This is done by plotting the variation of the velocity components along the circumference direction for selected values of r and z . This variation is compared to the corresponding value obtained from the axisymmetric data, which is an average value within the circumference. It is noticed that the variation of the 3-D data within the circumference is relatively small. No significant difference is shown between the peak points and the axisymmetric value within the circumference.

As a demonstration, the variations of the tangential component along two circumferences are shown in Fig. 5. The two circumferences are located at a radial distance $r = 158$ (m) and correspond to elevations $z = 28$ (m) and 10 (m), respectively. The plot shows the relatively small variation of the velocity values compared to the mean (axisymmetric) value. For $z = 28$ (m), the 3-D data varies between 139 (m/sec) and 145 (m/sec), while the corresponding axisymmetric value is 142 (m/sec).

Similarly, the variation of the radial component along the circumference is shown in Fig. 6 for radial distance $r = 158$ (m) and $z = 5$ (m). The difference between the 3-D values along the circumference to the mean (axisymmetric) value, shown in Fig. 3, is relatively small.

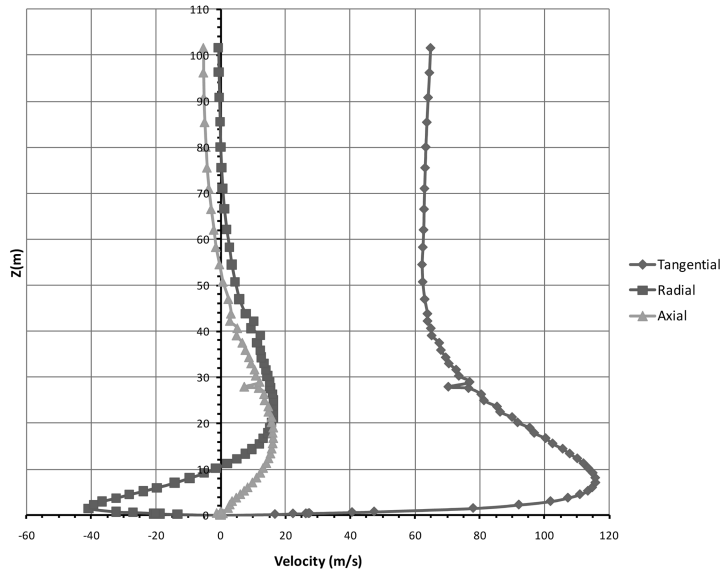


Fig. 4 Variation of the three velocity components of F4 tornado along the height at $r = 100$ (m)

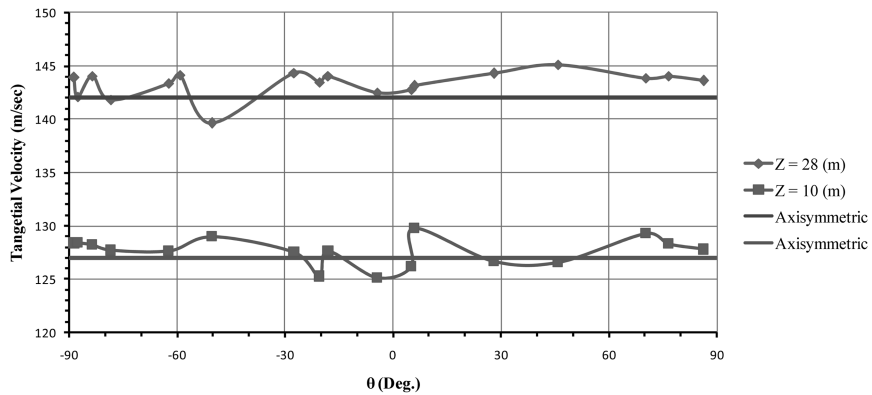


Fig. 5 Variation of the tangential velocity component along two circumferences at $r = 158$ (m)

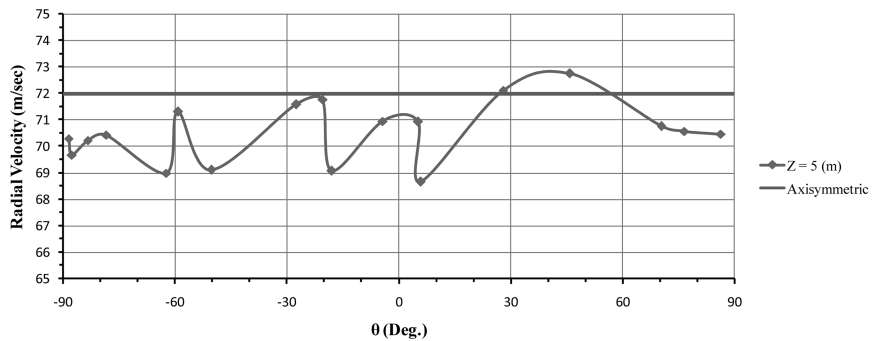


Fig. 6 Variation of the radial velocity component along two circumferences at $r = 158$ (m)

4. F2 – Tornado wind field

Unfortunately, no field data measurements are available in literature for F2 tornadoes. This is despite the fact that 86% of categorized tornadoes are associated with F2 tornadoes or less as stated by the ASCE No. 74 guidelines (1991). With the lack of field data, the following procedure is employed to estimate a velocity field for F2 tornadoes from the CFD data:

- 1- Based on the ASCE No. 74 guidelines (1991), the gust wind speeds of F4 and F2 tornadoes are 116 (m/sec) and 70.2 (m/sec), respectively. Accordingly, the ratio between the F4 and the F2 gust wind speed is $\frac{116}{70.2} = 1.65$.
- 2- The field measurements of F4 tornado predicted a maximum tangential velocity of 142 (m/sec). Accordingly, an estimate of the maximum tangential velocity for the F2 tornado is $\frac{142}{1.65} = 86$ (m/sec).
- 3- As reported in Section (3), a velocity scale $V_s = 13$ is established between the CFD data and the field measurements. This scale factor is applied to the set of data corresponding to various swirl ratios of 0.1, 0.4, 0.7, 0.8, 1 and 2. The maximum tangential velocity associated with the scaled values of different swirl ratio data is compared to the value of 86 (m/sec) estimated for the F2 tornadoes.
- 4- The comparison indicates that a swirl ratio $S = 1$ gives the best agreement with the maximum tangential velocity 86 (m/sec) estimated for the F2 tornadoes.
- 5- Accordingly, the set of data associated with $S = 1$ is used to simulate F2 tornadoes, together with the previously established scale factors $V_s = 13$ and $L_s = 4000$.

The peak values of the three components of the resulting wind field and their locations are provided in Table 1. Similar to the F4 wind field, the peak value of the three components occur at different locations.

The F2 tornado velocity profile has the same characteristics as the F4 profile described earlier with different values. Also, the locations at which the peak values occur are different between the F2 and F4 tornado fields. As a demonstration, the vertical profiles of the three velocity components for $r = 100$ (m) and $r = 50$ (m) are provided in Figs. 7 and 8, respectively.

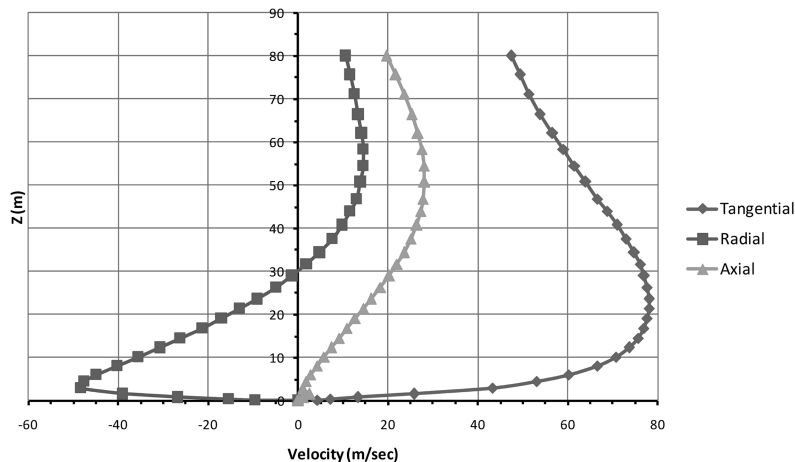


Fig. 7 Variation of the three velocity components of F2 tornado along the height at $r = 100$ (m)

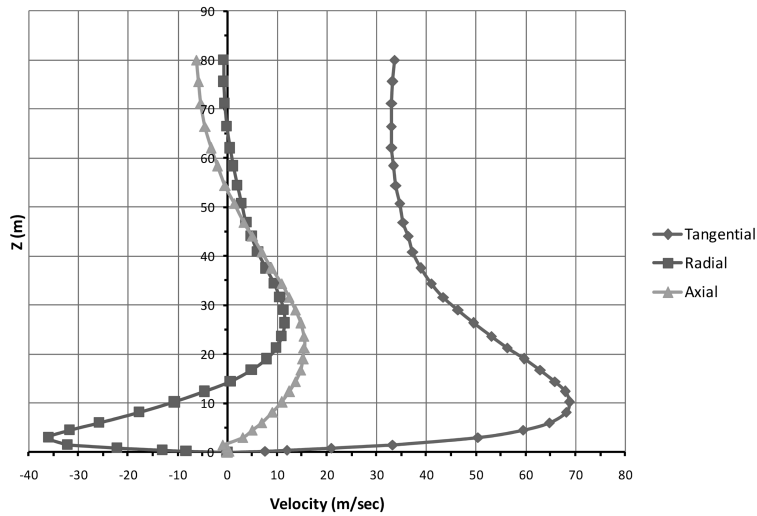


Fig. 8 Variation of the three velocity components of F2 tornado along the height at $r = 50$ (m)

5. Evaluation of the tornado velocity components at arbitrary location in the tower and conductors

The horizontal projection of a transmission tower is shown in Fig. 9. The following steps are conducted to evaluate the tornado velocity components at the arbitrary point “a” shown in the figure:

- 1- The centre of the tower (point 0) is considered the origin of the set of axes used in the

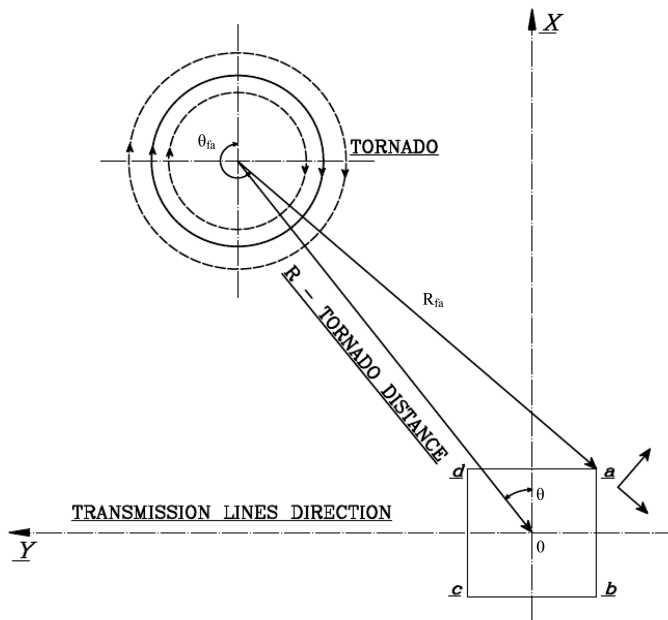


Fig. 9 Horizontal projection of transmission tower and tornado

analysis. The location of the centre of the tornado relative to the centre of the tower is defined by the polar coordinates R and θ . An assumption is made regarding the location of the tornado and, consequently, the values of R and θ . Knowing R and θ and the coordinates of point “a”, the coordinates R_{fa} and θ_{fa} , shown in Fig. 9, can be evaluated. They present the polar coordinates of point “a” relative to the centre of the tornado. In the view of the geometry of the tower, the vertical coordinate of point “a” is known and is identified by the variable Z_{fa} .

- 2- Based on the established value for the length scale $L_s = 4000$, the following equations can be used to obtain the model coordinates R_{ma} and Z_{ma} corresponding to R_{fa} and Z_{fa} , respectively.

$$R_{ma} = R_{fa} / 4000$$

$$Z_{ma} = Z_{fa} / 4000$$

Meanwhile, the model coordinate θ_{ma} remains the same as the full scale value θ_{fa} .

- 3- Knowing R_{ma} , Z_{ma} and θ_{ma} , the 3-D set of data can be used to obtain the model radial velocity V_{rma} , tangential velocity V_{tma} , and axial velocity V_{ama} components. However, the values of R_{ma} , Z_{ma} and θ_{ma} might not coincide with any of the coordinate values at which the CFD data is provided. Accordingly, a three-dimensional linear interpolation scheme is conducted between the CFD data points to obtain the values of V_{rma} , V_{tma} and V_{ama} .
- 4- Based on the established velocity scale $V_s = 13$, the corresponding full scale velocity V_{AX} , V_{RD} and V_{TN} are given by :

$$V_{AX} = V_{ama} \times 13$$

$$V_{RD} = V_{rma} \times 13$$

$$V_{TN} = V_{tma} \times 13$$

The evaluation of the velocity components is conducted in a similar way for the axisymmetric data, with less computational effort since the variation with “ θ ” is eliminated.

6. Description of the transmission line system

Manitoba Hydro transmission tower type A-402-0 is chosen as a generic guyed tower to study the behaviour of transmission towers under F4 and F2 tornado loads. A photograph of the considered line system is provided in Fig. 10. The tower is supported using four guys, which are connected to the tower using two cross-arms, located at an elevation of 35.18 (m). Four conductors hang between every two consecutive towers, two from each side, with an average span of 480 (m). The conductors are connected to the tower using insulators that are allowed to swing in two perpendicular planes. One ground-wire is attached to the top of the towers for lightning protection. The geometry of the towers is shown in Fig. 11. The total height of the tower is 44.39 (m), with conductors attached at an elevation 38.23 (m). The material and geometric properties of the conductors, ground-wire, guys and insulators are provided in Shehata *et al.* (2005)

7. Finite element modelling of transmission line/tower

The tower, conductors, ground-wire, guys and insulators are modelled using the finite element commercial program SAP2000 (CSI 2008). Details of the model are discussed below.

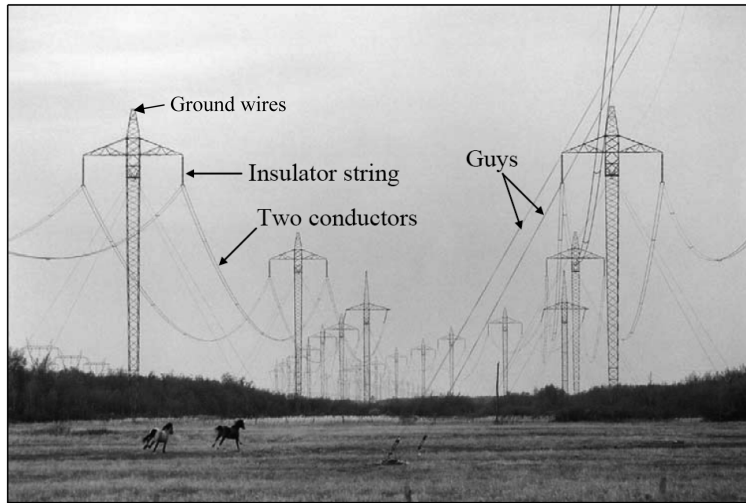


Fig. 10 Transmission line system (Source: Manitoba Hydro Company, Canada)

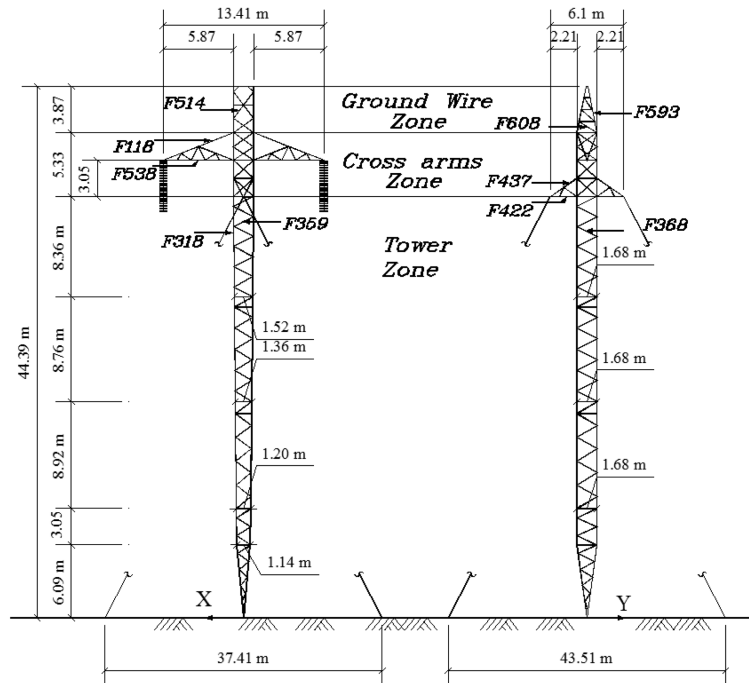


Fig. 11 Geometry of the modelled guyed tower type A-402-0

7.1 Tower modelling

A two-node non-linear three dimensional frame element with three translation and three rotational degrees of freedom per node is used to model the tower members. Each tower member is modelled using one element. Rigid connections are assumed between the tower members. This assumption is

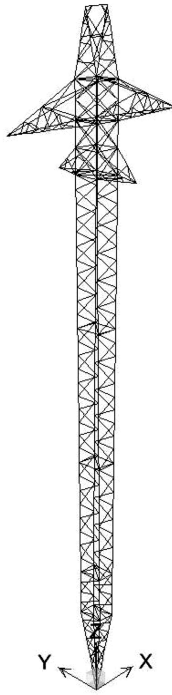


Fig. 12 Three dimensional tower model with global coordinate system

used to simulate the multi-bolted connections that are capable of transferring moments. The global coordinate system used in the simulation is shown in Fig. 12. The Y axis is along the direction of the conductors, the X axis is perpendicular to the conductors, and the Z axis is the vertical direction. Five towers and the in-between conductors and ground-wire are included in the model. The intermediate one is the tower of interest and the other 4 towers are considered to simulate the exact stiffness of the entire system. The model includes three cable spans from each side of the tower of interest. It was shown by Shehata *et al.* (2005) that such a number of cable spans provides an accurate prediction for the cable reactions transferred to the intermediate tower.

7.2 Conductors, ground-wire and guys modelling

The conductors, the ground-wire and the guys exhibit a highly nonlinear behaviour. A non-linear three dimensional cable element is used to model these components. This element uses an elastic cable formulation to simulate the behaviour of slender cables under the effects of self-weight, pretension force and external wind loading. Tension stiffness, sagging, and the geometric nonlinearities, resulting from large displacements and the P-delta effect, are included in the element formulation. The cable element has two nodes with three translation degrees of freedom at each node. The target pretension force of the cable is defined, and then nonlinear iterations are conducted to achieve this target pretension force. The stiffness matrix of the cable is calculated at the end of this load increment. This stiffness matrix takes into account the tension stiffening resulting from the pretension force. The subsequent load increment involves the application of the tornado wind loads. Each cable span is divided into thirty cable elements.

7.3 Insulator strings modelling

Each insulator acts as a three dimensional pendulum. The insulators are modelled using two-node three dimensional truss elements with three translation degrees of freedom at each node. One element is used to model one insulator. An intermediate hinge is assumed at the connection between the insulators and the tower cross-arms, allowing the insulators to rotate freely in two perpendicular planes.

8. Evaluation of forces on transmission tower and cables

The steps conducted to evaluate the tornado forces acting on the tower and the conductors associated with the tornado wind field are discussed below.

8.1 Forces acting in horizontal plane

The wind force acting on a nodal point of the tower in a certain direction “i” is calculated using the following equation provided in the ASCE No. 74 guidelines (1991).

$$F_{wi} = \frac{1}{2} \rho_a (Z_v V_i)^2 G C_f A \quad (3)$$

Where F_w is the wind force in “i” direction (N), ρ_a is the air density = 1.225 (kg/m³); Z_v is the terrain factor; V_i is the tornado velocity component in “i” direction (m/sec); A_i is the projected area of all the elements connected to the considered node and perpendicular to the “i” direction; G is the gust response factor and C_i is the drag force coefficient. The value of G , and Z_v , are taken equal to 1 as recommended by the ASCE No. 74 guidelines (1991). A value of C_i equal to 1 is assumed for the conductor as specified in the ASCE No. 74 guidelines (1991) and ANSI (1993). For the tower, the values of C_i are obtained from Table 2.6-1 of the ASCE No.74 guidelines (1991).

Fig. 13 shows a typical horizontal diaphragm of a transmission tower. The steps conducted to calculate the tornado forces acting on the nodal points a, b, c and d are presented below:

1. The tangential V_{TN} and Radial V_{RD} components of the wind load are evaluated at points a, b, c and d as illustrated before.
2. The velocity components V_{RD} and V_{TN} are resolved to evaluate the velocity components V_x and V_y acting along the cartesian coordinates for the four points a, b, c and d.
3. Average velocities V_x' and V_y' are calculated for the four points along the X and Y directions, respectively.
4. In view of Eq. (3), the force F_x and F_y acting along X and Y directions are given by

$$F_x = \frac{1}{2} \rho_a (V_x')^2 C_{fx} A_x \quad (4)$$

$$F_y = \frac{1}{2} \rho_a (V_y')^2 C_{fy} A_y \quad (5)$$

Where A_x and A_y are the projected area of all the elements connected to the considered node and perpendicular to the X and Y directions, respectively. The force coefficients in the X direction is calculated using the average of the force coefficients at the windward nodes of each

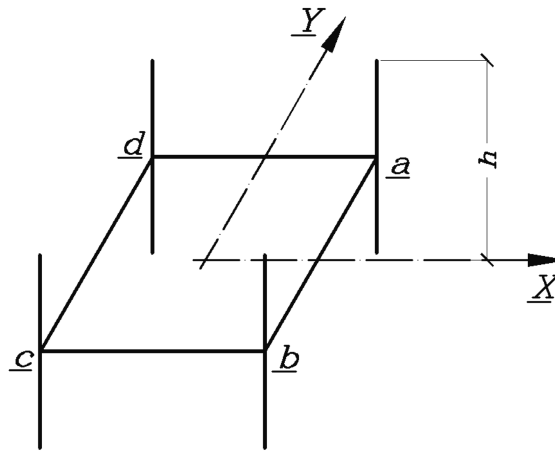


Fig. 13 Typical horizontal diaphragm of transmission tower

direction. A similar step is done for the Y direction to calculate C_{fy} .

5. The forces F_x and F_y are distributed between the windward and leeward faces using the shielding factor K , given in NBCC (2005).
6. The force components on the windward and leeward faces are distributed between the nodes on each face based on the projected area served by each node.

A similar procedure is used to obtain the nodal forces acting on the conductors, ground-wire and guys.

8.2 Forces acting in vertical plane

The tower is divided into a number of segments; each segment is bound by two consecutive horizontal diaphragm of the tower. The sequence of distribution of loading depends on whether the vertical velocity is acting upward or downward.

For the downward case, the upper face of the segment is considered the windward face, while the lower face is considered the leeward face. The calculations start by evaluating the force acting on the top segment. First, the vertical forces acting on the top of the tower are calculated using the same procedures employed for the evaluation of the horizontal forces, with the exception of using the axial velocity instead of the radial and tangential velocities. These top forces are distributed between the upper and lower face of this top segment using the shielding factor “K”. The calculations proceed by considering the second top segment. The forces acting on the lower face of the top segment are now considered as the total force acting on the second top segment. Distribution takes place, once again, between the upper and lower face, as conducted for the top segment. The same steps are conducted progressively for various segments until the ground level is reached. For the upward case, the same steps are conducted, starting from the ground level until the top of the tower is reached. In this case, the lower face of the segment is considered as the windward face, while the upper face is considered as the leeward face.

The nodal vertical forces F_z for the conductors, the ground-wire and the guys are calculated by applying Eq. (4). The value C_{fx} is replaced by $A_x = 1.0$ and A_x by A_z , which is the projected area of the lines in the plane perpendicular to the Z-direction.

9. Steps of analysis

The following steps are conducted to evaluate the response of a tower due to a specific tornado configuration:

1. The tower, the conductors, the ground-wire and the guys are modelled as described in Section (7). In addition to the tower of interest, two towers from each side of this specific tower are considered in the numerical model. The model includes five towers and six bays for each conductor, spanning between the five towers and the end hinged supports (see Fig. 14 for illustration). Each tower member is modelled using a frame element, while thirty cable elements are used to model each conductor and ground-wire span.
2. The CFD data of the tornado model (either F4 or F2) is retrieved and stored.
3. A tornado configuration, i.e., its location relative to the centre of the tower of interest, is assumed based on selected values for the parameters R and θ shown in Fig. 9.
4. The procedure described in Section (5) is adopted to evaluate the tangential, radial and axial velocity components at the nodal point of the tower of interest, and of the nodal points of the conductors, the ground-wire and the guys as well.
5. The horizontal and vertical forces acting on the nodal points are evaluated using the procedures outlined in Section (8).
6. A set of static, elastic and geometric nonlinear analysis is conducted for the transmission line as described below. The internal forces that develop in various members of the tower of interest due to the considered tornado configuration, are evaluated.

10. Case study

The transmission line system described in Section (6) is analyzed under tornado loading following the procedure outlined in the previous section. Two sets of analysis are conducted using both the axisymmetric and the 3-D F4 tornado data. A comparison is carried out between the internal forces developing in selected members of the tower using these two sets of data. Another set of analysis is conducted using the 3-D F2 tornado data. A comparison is conducted between the internal forces associated with the F4, F2 tornadoes and those resulting from normal wind loads evaluated based on the ASCE No. 74 guidelines (1991).

For the two tornado scales (F2 and F4), three analyses are conducted using a fixed value for the distance R and three different values for the angle θ of 0° , 45° and 90° , respectively. The values of R are taken equal to 158 (m) and 96 (m) for the F4 and F2 tornado, respectively. These values

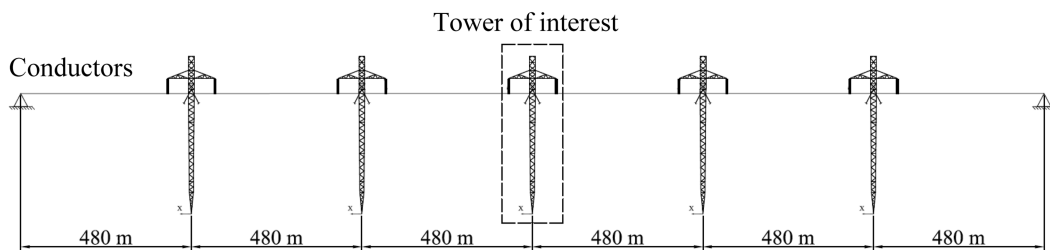


Fig. 14 Transmission line system

correspond to the location leading to the peak tangential velocity value at the tower of interest.

11. Results of the analysis

The results of the nine conducted nonlinear analysis are presented for some selected members of the tower of interest. As shown in Fig. 11, the tower is divided into three zones. The tower zone is located below the supporting guys. The cross-arm zone and the ground-wire zone are located at the upper part of the tower. For the tower and the ground-wire, the results are presented for one chord and two diagonal members, labelled as diagonal (1) and diagonal (2), respectively. Diagonal (1) and diagonal (2) are members located in plans parallel and perpendicular to the transmission line, respectively. The results of the analyses are provided in Table 2.

For each set of analysis, the absolute maximum (tension) or minimum (compression) values resulting from the three “0” configuration are provided for each member. The values of “0” corresponding to these critical values are given in Table 2. The internal forces reported in the table, associated with normal wind loads, are calculated using 10 (m) reference wind velocity of 32.6 (m/sec), which is believed to be the wind speed used in designing this transmission line. The following observations can be drawn from the results reported in the table:

- The difference between the results obtained using the 3-D and the axisymmetric data is small. It does not exceed 15% for all the reported cases.
- The F4 tornado leads to internal forces that are significantly higher than those resulting from the F2 tornado. This indicates that it might not be practical to design the tower members to resist an F4 tornado. It is known that F2 accounts for 86% of categorized tornadoes.
- The ratio of the peak axial forces reported in Table 2 under F4 and F2 tornado wind fields is between 2 to 20, while the ratio between the maximum tangential velocity of F4 tornado and

Table 2 Axial forces in selected tower members

Member		F4 Tornado (Axisymmetric CFD)		F4 Tornado (3-D CFD)		F2-Tornado (3-D CFD)		ASCE*	
		Axial Force (kN)	θ°	Axial Force (kN)	θ°	Axial Force (kN)	Axial Force (kN)		
Tower Zone	F318	Chord	-657	0	-638	0	-75	34	
	F368	Diagonal(1)	-61	0	-59	0	-3	3	
	F359	Diagonal(2)	-106	90	-95	90	-6	1	
Cross- arms Zone	Guy	F437	Upper Chord	516	90	468	90	59	17
		F422	Lower Chord	-400	90	-362	90	-44	31
		Guys		526	90	480	90	50	26
	Conductor	F118	Upper Chord	46	45	52	45	30	25
		F538	Lower Chord	-67	45	-72	45	-40	39
Ground- Wire Zone	F593	Chord	-70	0	-72	0	-18	2	
	F608	Diagonal(1)	8	0	5	0	1	1	
	F514	Diagonal(2)	17	0	17	0	5	1	

ASCE* The reported values represent the absolute peak forces

F2 tornado is only 1.85. The reason behind this difference can be explained as follows:

- The selected members reported in Table 2 are located at an elevation of 31 (m) relative to ground. At this location, the tangential velocity for F4 reaches its maximum value and remains then almost constant till the top of the tower. On the other hand, the maximum tangential velocity for F2 is located at an elevation of 19 (m) and decreases beyond this elevation. This difference in the vertical profile of the two velocity fields leads to a significantly larger effect for the F4 tornado.
- The portion of the conductors loaded during the F4 tornado is significantly larger than the portion loaded during the F2 tornado. This effect increases the overall forces acting on the tower during the F4 tornado.
- The F2 tornado produces internal forces that are higher than those calculated under normal wind loads.
- For chord members located in the main body of the tower (tower zone and ground-wire zone), the peak forces occur at $\theta = 0^\circ$, i.e., when the tangential components of the tornado wind field are parallel to the line direction.
- For diagonal members located in the main body of the tower (tower zone and ground-wire zone), the peak values for diagonal (1) and diagonal (2) occur when the tangential components of the tornado wind field are parallel to the member vertical plane.
- For the supporting guys shown in Fig. 11, the peak forces occur at $\theta = 90^\circ$, i.e., when the tangential components of the tornado wind field are perpendicular to the line direction. This case leads to a maximum value for the tangential forces acting on the tower. In addition, under this tornado configuration, the two adjacent spans are almost fully loaded, which increases the guys forces.
- For some members in the cross-arm zone, the peak forces occur at $\theta = 45^\circ$. This configuration produces unbalanced forces on the conductor spans adjacent to the tower, leading to a resultant longitudinal force in the conductors. Such a force leads to an out-of-plane bending effect in the cross-arms, which creates large force in the chord members in this region. Similar behaviour was reported by Shehata and El Damatty (2007) when they studied the tower behaviour under downbursts.

12. Conclusions

A numerical scheme for evaluating the response of transmission line structures to tornado loading is developed in this study. The tornado wind field is based on a computational fluid dynamic (CFD) model that was developed and validated experimentally in a previous study. The CFD data, together with the tornado field measurements and the information provided in the design codes, are used to establish the wind field associated with F4 and F2 scale tornadoes. The procedure used to obtain the wind loads due to the tangential, radial and axial velocity components of the wind field is described. A three-dimensional finite-element model for a transmission line system is developed. The model focuses on evaluating the response of one of the guyed towers of the system to tornado loads. The model includes a simulation for the tower of interest, in addition to two towers and three spans for the conductors, and the ground-wire from each side of the tower of interest. The analysis is carried out in a static, elastic and geometric nonlinear manner by including the effects of conductors' pretension, sagging, secondary moment and large displacements.

A set of analysis is conducted under F4 scale tornado assuming that the tornado is located at the

position leading to maximum tangential velocity at the tower of interest. The analysis is carried out using both axisymmetric and three-dimensional sets of tornado fields. The analysis is also repeated using a three-dimensional F2 tornado field, where the tornado is also assumed to be located at the position leading to maximum tangential velocity at the tower of interest. The following conclusions can be stated from the analyses conducted in the study:

- The vertical profiles of the F4 and F2 tornado fields have patterns that are different than the conventional boundary wind profile.
- The internal forces obtained from the analysis conducted using three-dimensional CFD data do not significantly differ than those obtained using the axisymmetric CFD data. The maximum difference is less than 15%.
- The peak values of the axial forces in the tower of interest are sensitive to the relative location between the centre of the tornado and the tower.
- The internal axial forces under F4 tornado are significantly higher than those resulting from the F2 tornado.
- The peak values of the axial forces resulting from the F2 tornado wind field are higher than the values resulting from normal wind load with reference velocity 32.6 (m/sec).

In light of these findings, it can be concluded that it is important to consider the tornado loads when designing a transmission line system. This definitely depends on the risk of occurrence of tornadoes at the location of the line. Further investigations are needed in order to understand the behaviour of various transmission line systems under tornadoes. These studies can ultimately lead to the development of a set of patch loading simulating the effect of tornadoes.

References

- American National Standards Institute (ANSI) (1993), *National Electrical Safety Code (NEC)*, Accredited Standards Committee C2, USA.
- American Society of Civil Engineers (ASCE) (1991), *Guidelines for electrical transmission line structural loading (ASCE Manuals and Reports on Engineering Practice)*, No. 74, NY.
- Baker, D.E. (1981), *Boundary layers in laminar vortex flows*, Ph.D. thesis, Purdue University.
- Chay, M.T., Albermani, F. and Wilson, R.J. (2007), "Response of a guyed transmission line tower in simulated downburst winds", *Proceedings of the 12th International Conference on Wind Engineering (ICWE12)*, Cairns, Australia, July.
- Computer and Structures, Inc. (2008), *SAP2000 V.12, CSI Analysis Reference Manual*, Berkeley, California, USA.
- Fluent Inc. (2005), *Fluent 6.2 User's Guide*, Lebanon.
- Hangan, H. and Kim, J.D. (2008), "Swirl ratio effects on tornado vortices in relation to the Fujita scale", *Wind Struct.*, **11**(4), 291-302.
- Lee, W.C. and Wurman, J. (2005), "Diagnosed three-dimensional axisymmetric structure of the Mulhall tornado on 3 May 1999", *J.Atmos.Sci.*, **62**(7), 2373-2393.
- National Research Council Canada (2005), *National Building Code of Canada 2005*, Associate Committee on the National Building Code, Canada.
- Sarkar, P., Haan, F., Gallus, Jr., W., Le, K. and Wurman, J. (2005), "Velocity measurements in a laboratory tornado simulator and their comparison with numerical and full-scale data" *Proceedings of the 37th Joint Meeting Panel on Wind and Seismic Effects*, Tsukuba, Japan, May.
- Savory, E., Parke, G.A.R., Zeinoddini, M., Toy, N. and Disney, P. (2001), "Modelling of tornado and microburst-induced wind loading and failure of a lattice transmission tower" *Eng. Struct.*, **23**(4), 365-375.
- Shehata, A.Y., and El Damatty, A.A. (2008), "Failure analysis of a transmission tower during a microburst" *Wind*

- Struct.*, **11**(3), 193-208.
- Shehata, A.Y. and El Damatty, A.A. (2007), "Behaviour of guyed transmission line structures under downburst wind loading", *Wind Struct.*, **10**(3), 249-268.
- Shehata, A.Y., El Damatty, A.A. and Savory, E. (2005), "Finite element modelling of transmission line under downburst wind loading" *Finite Elem. Anal. Des.*, **42**(1), 71-89.
- Wurman, J. (1998), "Preliminary results from the ROTATE-98 tornado study", *Proceedings of the 19th Conference on Severe Local Storms*, Minneapolis, MN, USA, September.

JH